Materials Research. 2022; 25:e20220411
DOI: https://doi.org/10.1590/1980-5373-MR-2022-0411

Determination of Copper and Iron in Real Sample of Water and Ethanol Using Square Wave Voltammetry with a Micro/Nano Boron-Doped Diamond Electrode

A. C. S. Ibernom[a], *N. G. Ferreira*[b], *N. A. Braga*[a]*

[a]*Universidade Federal do Amazonas, Departamento de Química, Manaus, AM, Brasil.*
[b]*Instituto Nacional de Pesquisas Espaciais, Laboratório de Sensores e Materiais, São José dos Campos, SP, Brasil.*

Received: September 13, 2022; Revised: December 08, 2022; Accepted: February 01, 2023

Currently, the search for a more economical alternative with adequate selectivity, sensitivity and reproducibility in the determination of metallic ions is important for the development of reliable methodologies for the determination of these contaminants. This work investigates a boron-doped micro/nano diamond electrode, with different morphology and structure compared to those discussed in the literature, for the detection of copper and iron in aqueous and ethanolic environments. Internal validation of the Square Wave Voltammetry was applied. The methodology was submitted to validation by: selectivity, linearity, precision (interday test), accuracy (percentage of recovery) and detection and quantification limits. The results indicated that this type of electrode showed good response to determinations in aqueous and ethanolic environments, with good selectivity, linearity, accuracy (recovery between 70% and 110%) and precision, presenting the best detection and quantification limits for the aqueous. The methodology using a boron-doped diamond micro/nano electrode was suitable for the determination of copper and iron metals in both matrices.

Keywords: *Boron-doped diamond, morphology, structure, methodology, metal detection, validation.*

1. Introduction

Numerous toxic metals are released into the environment through industrial activities every year. It is necessary to monitor its presence in different matrices and ecosystems[1] since metals as copper and iron, can interfere with the nervous, gastrointestinal, cardiovascular, renal and hematopoietic systems in humans and other animals, even at low concentrations.

The analytical methods traditionally used to quantify these metals are atomic absorption spectrometry[2], molecular absorption spectrophotometry[3], among others[4]. Despite the versatility, sensitivity and efficiency of these methodologies, they have the disadvantage of sophisticated and expensive instrumentation. Electrochemical methods have been employed for the determination of compounds at trace levels in industrial[5], biological[6] and environmental[1,7] product monitoring studies with adequate sensitivity, precision and accuracy. Such electrochemical methods use a working electrode that favours the analytical degree of detections in real samples.

Boron-doped diamond (BDD) electrodes appear a material, with advantages that correspond to their low background current; wide window of potential; extraordinary morphological and structural stability at high temperatures; good response to some aqueous and non-aqueous analytes without conventional pretreatment[8]. These properties favoured the evolution of the use of diamond as a working electrode to detect a variety of analytes, including trace heavy metals[9]. However, there is no studies in the literature regarding the use of Square Wave Voltammetry (SWV) with electrodes of mixed micro/nano BDD morphology for the determination of copper and iron metals in real samples of water and fuel ethanol. Thus, it is important to develop and validate a voltammetric method that uses a new electrode to detect these metals.

It is recognized that an analytical method before being used in quality control or by regulatory bodies should be validated. To do so, it must present comparability, traceability, and reliability in chemical measurements, proving its adequacy to the intended purpose[10]. The validation of analytical methodologies for the analysis of emerging pollutants in environmental samples has made use of different validation strategies, described in INMETRO[11] and in the literature[12]. In the present work, a laboratory validation study was developed for quick, simple and low-cost quantification of copper and iron metals in aqueous and ethanolic media using an electrode containing a mixed morphology that until now has not been addressed in the literature.

2. Methodology

2.1. Characterization of BDD film

The BDD film were obtained by the technique of chemical deposition from the activated gas phase in a Hot Filament Chemical Vapor Deposition (HFCVD). Reactor film used in this work were obtained with a doping level of 15000 ppm,

*e-mail: neilabraga@ufam.edu.br

from a gaseous mixture of 160 sccm of argon, 38 sccm of hydrogen and 2 sccm of methane, for a deposition time of 18 hours, maintaining the substrate temperature in the range of 635ºC to 650ºC.

From the study of the morphological and structural characterizations of BDD film were performed using the techniques of Scanning Electron Microscopy (SEM), Atomic Force Microscopy (AFM), Raman scattering spectroscopy and X-ray diffractometry (XRD). SEM analyses were performed in a JEOL microscope model JSM-5310. AFM was obtained using a BRUKER microscope, model INNOVA, operating in contact mode with a temperature of 24ºC and relative humidity of 35%, using a silicon nitride tip. The Raman scattering spectrum was obtained using a microscope HORIBA Johin and Von MODELO M.F.O. The XRD of this study were obtained using a diffractometer PHILIPS X "PERT MRD.

2.2. Reagents

The solutions used in this study were prepared with reagents of analytical purity (AP) and the purified water was used in the Milli-Q system (18 MΩ cm^{-1}). The deaeration of the solutions in the voltammetric measurements was performed using 99.999% super dry nitrogen gas. All glass material used in the electrochemical experiments, such as electrochemical cells, volumetric flasks, and beakers, were previously washed with distilled water and left for 24 h in 10% (v/v) nitric acid and then washed with ultrapure water before use. All metal solutions were prepared using 1000 mg L^{-1} Sigma - Aldrich standards.

2.3. Electrochemical measurements

Electrochemical measurements were performed using an Autolab PGSTAT 302N Potentiostat/Galvanostat. An electrochemical cell with a conventional three-electrode system was used, a platinum wire as the counter electrode, and Ag/AgCl (3 M KCl) as the reference electrode, with a BDD film as the working electrode. The effective active area of the BDD was obtained by recording the CV (Cyclic voltammetry) test with different scan rates.

Concentrations of 10 mg L^{-1} of metallic species were used in all studies as a solution mother to validate the proposed methodology. The study used different electrolytes support for each medium, as shown in Table 1. The analyses with hydroalcoholic solutions were performed in the range of 20/80 v/v ethanol. The parameters of the SWV technique used for the validation of the methodology are highlighted in Table 1.

The analytical curves were obtained by the standard addition method in the concentration range of the metals Cu^{2+} and Fe^{3+} from 0.001 to 0.007 mg L^{-1} for real samples. To verify the performance of the electroanalytical methodology, the parameters of selectivity, linearity, accuracy, precision, limits of detection (LD) and quantification (LQ) were analysed according to recommendations of resolutions and articles in the literature[11,13-15].

The real samples were collected from igarapé of 40 and at different gas stations in the city of Manaus, Brazil, and then stored in polyethylene bottles and later diluted in the electrolyte support.

Table 1. Parameters SWASV adopted for the study of Figs of merit.

Parameters	Half Aqueous		Ethanolic Medium	
	Cu^{2+}	Fe^{3+}	Cu^{2+}	Fe^{3+}
Electrolyte support	KCl		H_2SO_4	HCl
	1.0		0.04	0.04
	mol L^{-1}		mol L^{-1}	mol L^{-1}
Frequency (*f*)	60	70	50	30
	Hz	Hz	Hz	Hz
Amplitude (*a*)	70	90	70	100
	mV	mV	mV	mV
Potential for deposition (E_{dep})	-0.2	-0.1	-0.4	
	V	V	V	
Deposition time (T_{dep})	60 s		60 s	
Equilibration time (T_{eq})	60 s		60 s	50 s

3. Results and Discussion

3.1. Morphological and structural characteristics

By means of the SEM image (Figure 1a) it was possible to observe that the BDD film was formed by diamond grains with randomly oriented crystals, having a rough surface with a microcrystalline grain morphology, as one can see such an image. These grains have pyramidal structure similar to the microcrystalline structure, but when the image is approximated (insert of Figure 1a) one can observe small crystals on its surface, as also approached by Rehacek[16] in his work, being characterized as a morphology that suffered renucleation with nanocrystalline diamonds (BDD micro/nano), thus having a roughness in its structure due to these renucleated grains. This can also be verified from the gas mixture during the growth of the BDD micro/nano film, in which it presented an insertion of argon gas in the mixture (160 sccm) that caused a consequent reduction in the concentration of hydrogen (H_2) when compared to films microcrystalline that do not have argon in their gas mixture. With little hydrogen reacting on the surface, the growth from different species is favoured, causing the renucleation process of the grains, which consequently also decreases their size[16,17]. In addition, the AFM images over an area of 20 x 20 μm^2 also allowed observation of the morphology of the film (Figure 1b), in which it was possible to confirm what was observed by SEM. By means of the AFM images, it was possible to calculate average, finding a value of 492.5 nm for this film, showing that it has a roughness higher than that of many electrodes used in electrochemistry[18]. These morphological characteristics favor the roughness of the film, which is an important factor in electrochemistry, since, as Pleskov[19] observed, electrodes with more rough surfaces are more reversible. The increase in roughness also implies an increase in the electrochemical area of the electrode resulting in an increase in the current response of the electrode[20].

The composition and amount of the phases present in the material, as were well as the crystallinity measurements investigated by XRD are shown in Figure 1c. They were obtained with the 2θ angles in the range of 30° to 80°. The diffractograms were analysed with some articles[7,9,20,21].

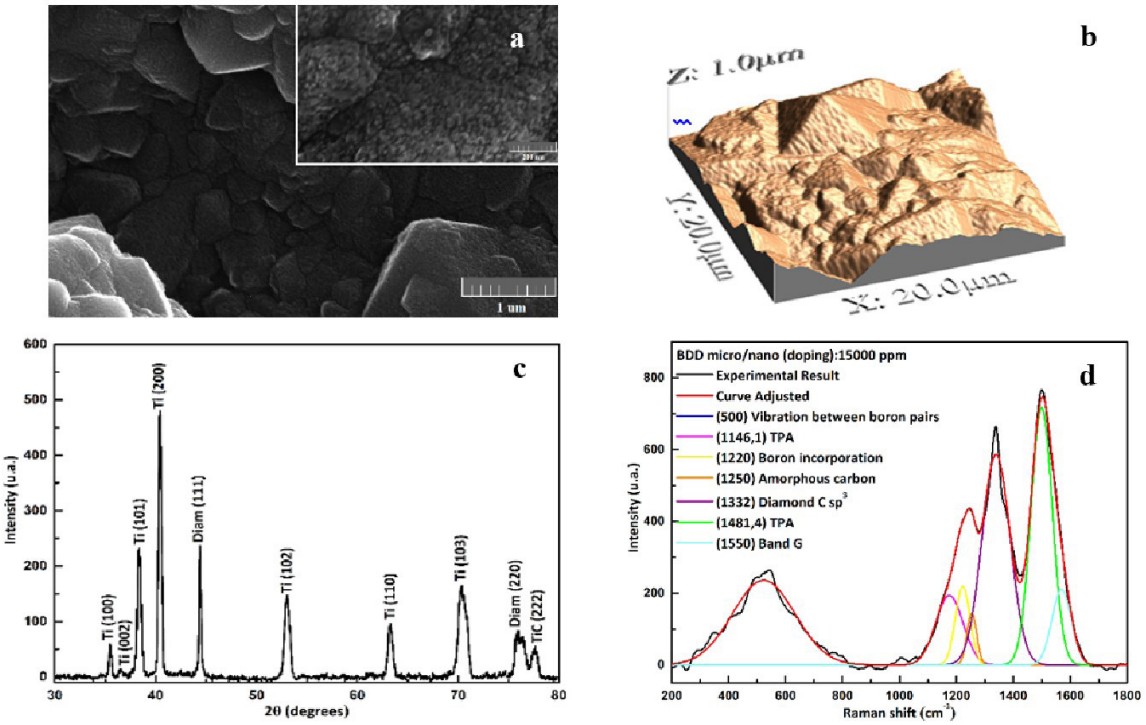

Figure 1. Morphological analysis images and graphs of the structural analysis of the BDD micro/nano electrode grown on titanium substrate with the doping level of 15000 ppm. (a) SEM; (b) AFM; (c) XRD; (d) Raman.

The XRD spectra show the formation of the Ti phases related to the peaks (100), (002), (101), (200), (102), (110) and (103) and the peak related TiC phase (220). The peaks from Ti/substrate are present in the diffractogram by the depth that the X-rays reach during the analysis.

The peaks at 2θ equal to 44° and 75.5° correspond to diffractions of the crystallographic plane of the diamond (111) and (220), confirming the presence of these phase in the material. These planes allow to observe that the intensity of the plane (111) of this film is close to that of microcrystalline films, presenting a lower intensity when related to them due to the influence of renucleated nanocrystalline grains in their structure, being confirmed by the intensity of the plane (220) when compared to data obtained in the literature[9,21] which is correlated with the process of decreasing grain size which also increases the amount of sp^2 carbon at the limits of the diamond grains.

In addition, these plans (111) and (220) provide valuable information about the films. With XRD it is still possible to determine the average grain size. According to Shi[22], small particles or crystallites will produce extensive diffraction domains in the reciprocal space. The diffraction domains are inversely proportional to the size of the crystallites, and this translates into an observable widening of the X-ray diffraction line. Considering that this enlargement is caused by the limited size of the nano renucleated grains, the Scherrer formula can be used to determine the mean grain size in the direction normal to the planes (hkl)[23].

The calculation of grain size by the width at half height of the diffraction peak, overestimates the actual value, because there is a size distribution, the larger grains will give a strong contribution in the intensity, while the smaller grains only widen the base of the peak[24,25]. In this way, the value found for grain size was 24.9 nm, due to a mixture of nano and micro morphologies in this film.

The Raman scattering spectrum (Figure 1d), obtained in a range of 200 to 1800 cm^{-1}, clearly shows the occurrence of the characteristic diamond phases in the deposited film. There is a Raman peak at 1332 cm^{-1} which is characterized as Raman signature for the diamond, corresponding to the vibration of the first order phonon of the material[26]. This peak is very evident and intense because the film presents microcrystalline grains in its morphology, being observed a small enlargement of this peak coming from the overlap of the D band (1326.4 cm^{-1}), a behaviour normally observed in films with nanocrystalline morphology for Raman excitations in the visible region[9]. This broadening of the peak that characterizes the diamond was already expected because the film has in its structure nanocrystalline renucleated grains. The doping of the film is verified through the bands at 500 cm^{-1} and 1220 cm^{-1} which are related to the modes of vibration of pairs of boron[26].

At 1550 cm^{-1} the peak of the G band corresponding to graphite[21] phase appears indicating the presence of sp^2 carbon. In addition, the peaks at 1146 cm^{-1} and 1481 cm^{-1} corresponding to the transpoliacetylene (TPA) present in the grain boundary tend to appear in samples having a large amount of argon in the mixture been identified only in nanocrystalline samples or with nano renucleated grains in their morphology[17]. The TPA favours semiconductor characteristics to the film by providing it a semimetallic behaviour.

The amount of substitutional boron was $1.12x10^{20}$ cm^{-3} for the BDD micro/nano. According to Rehacek[16], when boron is introduced in the film with a doping of the order of 10^{17} - 10^{20} cm^{-3} the diamond presents properties of a semiconductor (known as hopping). In this way, it is possible to frame the number of carriers with the type of electronic transport that occurs[19,20]. Such characteristics favour a conductive film even without boron doping.

Since TPA favours a semiconductor characteristic and by incorporating boron pairs in its structure, as shown by Raman, this film becomes highly conductive and with a favourable morphology and structure for the detection of trace metals. As proven by electrochemical characterization.

3.2. Electrochemical characteristics

The determination of the potential window (working range) of the electrode is a parameter that defines the region that allows the detection of oxy-reduction reactions. The potential window is obtained by applying a potential to the electrode in order to obtain the response. In positive potentials (anodic potential) there is formation of O_2 (Figure 2a), while in negative potentials (cathodic potential), there is H_2 formation (Figure 2a). The current signals generated from the cited reactions to the water can mask the current signal generated by any analyte which exhibits oxidation and reduction potentials in those regions, thereby limiting the possibilities of detection of the analyte. However, the BDD micro/nano electrode presents an intrinsic advantage that is the fact that the processes of oxidation and reduction of water occur in high potentials, thus extending the working range[9]. Thus, the section where the current tends to be zero, between these two reactions is called a potential window. BDD presenting a potential window of approximately 3V (2.75V).

Figure 2b shows the set of cyclic voltammograms obtained for the BDD micro/nano electrode. Each cyclic voltammogram was obtained by applying a potential difference in the range of -0.2 V to 1 V. Cyclic voltammograms were collected at different scanning rates in the range of 5 to 100 mV. The experiments were carried out in an electrochemical cell containing $K_4Fe(CN)_6$ 1 mmol L^{-1} solution in 0.5 mol L^{-1} H_2SO_4. In order to carry out the tests, the first applied potential was -0.2 V × Ag/AgCl, where it was possible to observe the occurrence of a small anodic current that approaches zero as the scanning proceeds. This initial current probably arises from the charge of the double electric layer[13].

From the current values obtained in the cyclic voltammogram the active area of the electrode was calculated using the Randles-Sevcik equation, finding an electrochemical area of: 0.11 cm^2 for the BDD micro/nano electrode. In this way, an increase of area of the electrode was verified in comparison with the geometric area (0.032 cm^2). These characteristics favour the roughness of the film, as evidenced by the AFM, which results in an active area larger than the geometric area of the film.

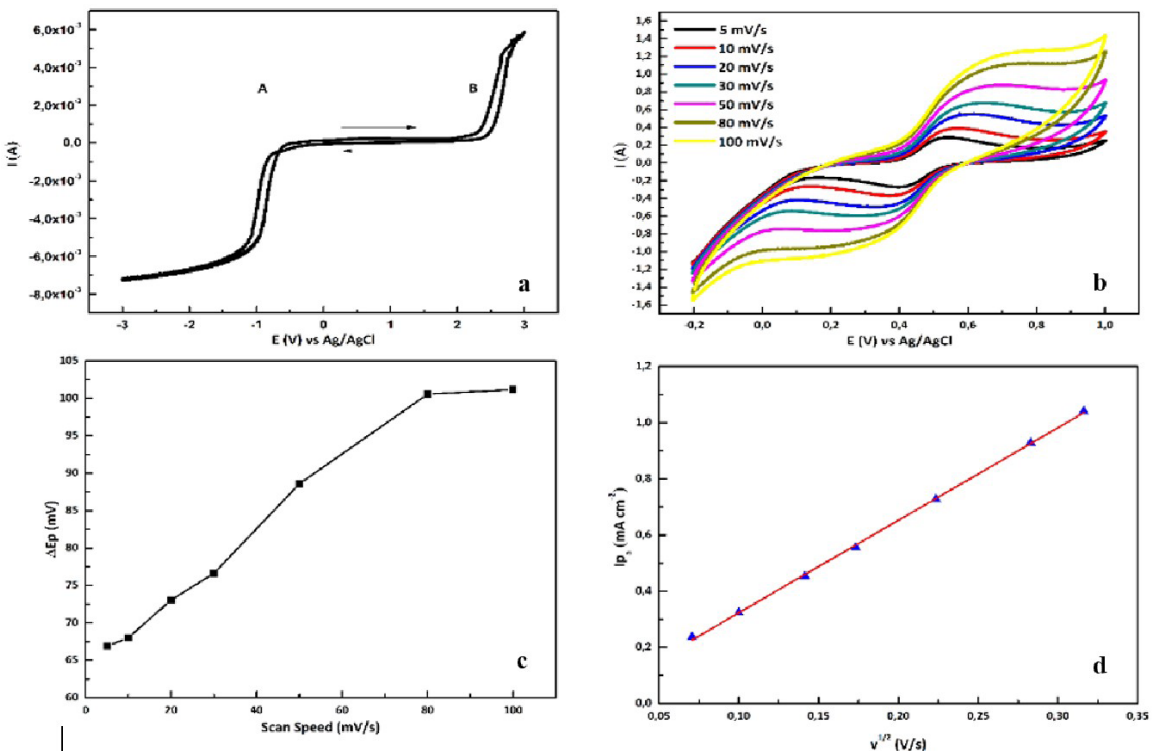

Figure 2. Electrochemical characterization. (a) Potential window for the BDD micro/nano electrode in H_2SO_4 0.5 mol L^{-1} using a potential range of -3 to +3V with a scanning speed of 30 mV s^{-1}; (b) Cyclic voltammograms of the redox system in 1.0 mmol L^{-1} $K_4Fe(CN)_6$ in H_2SO_4 0.5 mol L^{-1} obtained by Cyclic Voltammetry at a scanning speed of 5 to 100 mV s^{-1} for the BDD micro/nano; (c) Relation between ΔEp (ΔEp = Epc-Epa) and scanning speed of the electrodes obtained in solution 1.0 mmol L^{-1} of $K_4Fe(CN)_6$ in H_2SO_4 0.5 mol L^{-1}; (d) Relation between the anodic peak current density and the square root of the electrode sweep velocity obtained in solution of 1.0 mmol L^{-1} of $K_4Fe(CN)_6$ in 0.5 mol L^{-1} of H_2SO_4.

The graph shown in Figure 2c shows the variation of ΔE_p with the scanning speed (ν) for the BDD micro/nano film in solution of 1.0 mmol L^{-1} of $K_4Fe(CN)_6$ in 0.5 mol L^{-1} H_2SO_4. Demonstrating the Fig that ΔE_p increases as the scanning speed is increased. Extrapolation of the line in this graph shows that it walks to a value close to 60 mV at low scanning speeds. This shows that, in this condition, this electrode is close to a reversibility kinetics.

Another reversibility criterion applied to this electrode was presented in Figure 2d. The quasi-reversible behaviour is characterized when the anodic peak current density (I_{Pa}) increases as a function of the square root of the scanning velocity ($v^{1/2}$) proportionally to the electrode in ferrocyanide solution. By Figure 2d it is possible to observe that the linear increase of the anodic peak current density as a function of the square root of the scanning velocity was confirmed[16,27]. To conclude if the electrode presents kinetics of reversibility or near-reversibility

3.3. Validation of voltammetric methodology

The intra-laboratory validation study of the voltammetric method proposed in this study for the determination of Cu^{2+} and Fe^{3+} metals in water and ethanol was performed by evaluating the parameters of selectivity, linearity, precision, accuracy and limits of detection and quantification by different statistical techniques of resolutions and literature[13-16] recommendations.

The selectivity has the purpose of guaranteeing the identity of the analyte to be determined, being a measure of method indifference to the presence in the sample of species that could interfere in the determination of the analyte of interest. Selectivity ensures that the peak response is exclusively of the compound of interest.

In this work, the selectivity was evaluated using the standard addition method. This method is used when it is not possible to obtain the matrix (real sample) free of the substance of interest. In this case, two analytical curves of the metals (0.001 to 0.006 mg L-1 of Cu^{2+} and Fe^{3+}) were made, using SWV voltammograms of the oxidation peak of the species (Figure 3), each one without matrix effect, constructed from a standard solution of Cu^{2+} and Fe^{3+} and the statistical analysis of the F test. The results obtained for the study of the parallelism of the curves showed that for the studied metals both matrices presented good selectivity of the technique.

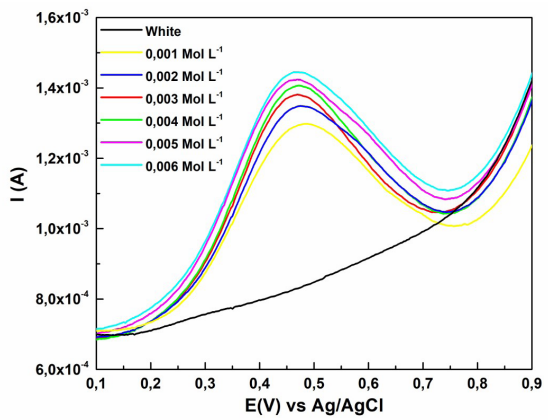

Figure 3. SWV voltammograms of the oxidation peak of the species Fe^{3+} in ethanol.

As can be seen in Figure 4, the respective curves are parallel to each other for the BDD micro/nano electrode and have coefficient of determination (R^2) greater than 0.99, thus guaranteeing the selectivity of the method. It is worth noting that even in the face of the occurrence of some points that are outside the curve when compared to the other points, there was no loss to the method selectivity parameter. In addition, the F test was performed to verify if there is a significant difference between the curves, obtained from the replicate variances of the concentrations of both analytical curves. Analysis of the results of the F test were obtained according to Table 2. Thus, as the F (calculated) < F (tabuled) the precision of the curves did not have a significant difference, which proves the guarantee of the selectivity.

The working range was evaluated in the range of 0.001 mol L^{-1} to 0.007 mol L^{-1} prepared in aqueous and ethanolic medium for the voltammetric quantification of Cu^{2+} and Fe^{3+} metals, using the parameters previously optimized by square wave voltammetry[13], following the same model in Figure 3.

The respective intensities of the peaks of the anodic redissolution voltammetry technique for the signals for the Cu^{2+} and Fe^{3+} ions were subjected to the least squares (LS) regression analysis, in order to construct external calibration curves for each analyte. From the generated curves, it was possible to establish the sensitivity (angular coefficient), the linear coefficient and the correlation coefficients (R) and determination (R^2) of the method developed for the selected analytes, as well as the statistical residues of each metal analysed in each matrix, in order to ascertain the quality of the analytical curves constructed[14]. The confirmation and acceptability of linearity depends on R^2, which is expected to be higher than 0.99, as well as a random distribution between positive and negative values of the residual points[15] from the LS regression. If this distribution is random, the graph does not present dispersion tendencies of the residues, being therefore an indication that the linearity is satisfactory[14].

Table 2. F-test for the study of selectivity in aqueous and ethanolic medium for BDD micro/nano.

F-test	
Average Variance of Et_{matriz} Cu^{2+}	$3.7228x10^{-9}$
Average Variance of Et_{PA} Cu^{2+}	$6.521x10^{-10}$
F (calculated)	5.708
Average Variance of Et_{matriz} Fe^{3+}	$1.9936x10^{-11}$
Average Variance of Et_{PA} Fe^{3+}	$4.8933x10^{-12}$
F (calculated)	4.074
Average Variance of H_2O_{matriz} Cu^{2+}	$1.5594x10^{-9}$
Average Variance of $H_2O_{deioniz}$ Cu^{2+}	$3.5641x10^{-10}$
F (calculated)	4.375
Average Variance of H_2O_{matriz} Fe^{3+}	$1.5347x10^{-11}$
Average Variance of $H_2O_{deioniz}$ Fe^{3+}	$2.7848x10^{-12}$
F (calculated)	5.510
$F^{4(N-1)}$ (tabulated)	6.388

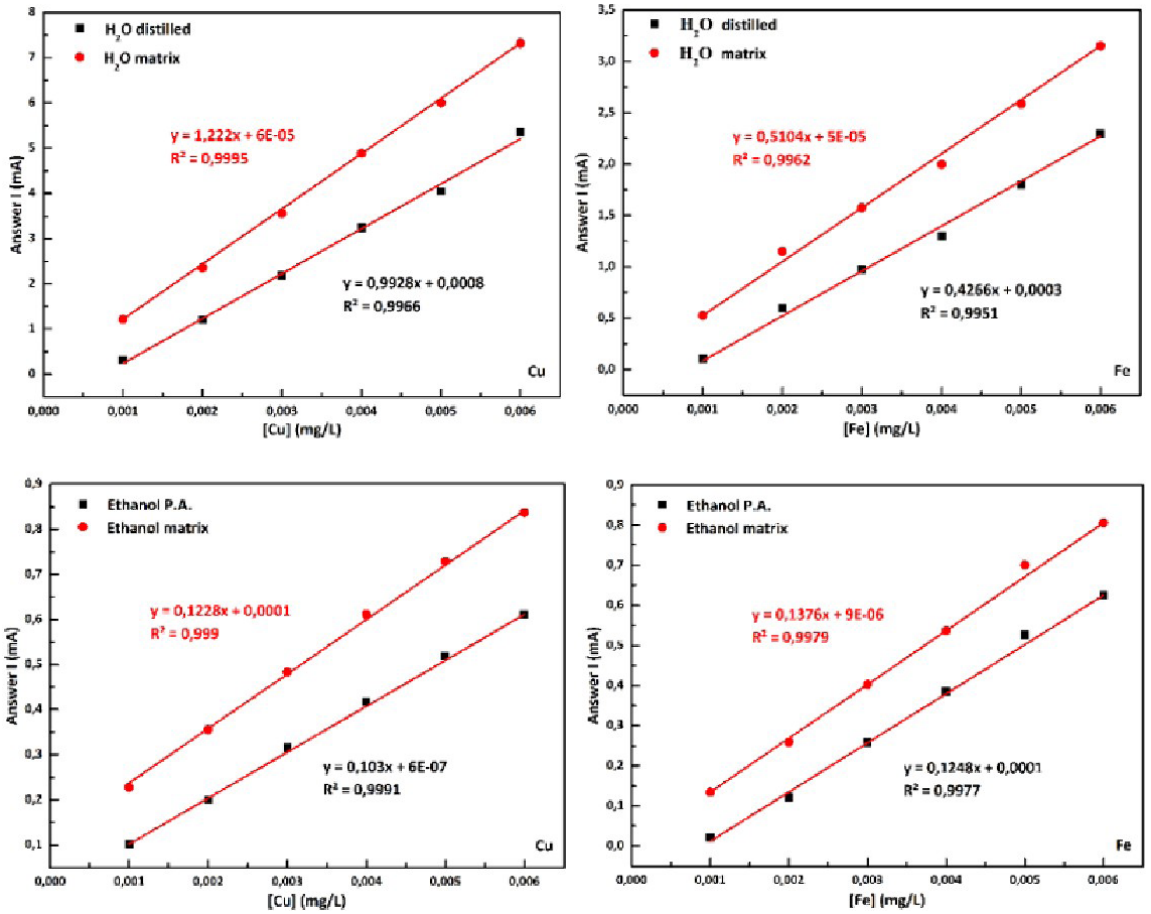

Figure 4. Analytical curves constructed from stock solution of copper (Cu^{2+}) and iron (Fe^{3+}) using a working range of 0.001 mg L^{-1} to 0.006 mg L^{-1} for aqueous and ethanolic medium, varying the electrochemical parameters.

The results obtained from the regression using the LS for the study of linearity can be observed in Table 3.

From the results obtained, it was observed by means of the visual analysis of the analytical curves as well as the scatter plots of statistical residues of the metals in aqueous and ethanolic medium, that they indicate that the linearity of the respective analytical curves were found to be satisfactory because, for all two metals, the R^2 is higher than 0.99 and the residual dispersions presented a random distribution pattern along the abscissa axis, as recommended by INMETRO[11].

Precision was assessed by repeatability estimates. Repeatability was calculated from three consecutive peak current measurements for the low, medium, and high concentrations of the working range. Table 4 and 5 expresses the final summary of the data resulting from each test performed in terms of coefficient of variation of the means and the Horwitz coefficient. The acceptability of the accuracy is conditioned to a CV of less than 10%[2] and as it can be verified, for the entire concentration range the calculated results were below 10% indicating that the method developed presents satisfactory repeatability and precision.

Similar to the precision test, the accuracy test occurred simultaneously with the linearity test. For each control concentration level, the percentages of recovery were determined from the regression data of their respective analytical curves and the mean intensities of their respective anodic redissolution peaks. In Table 6 and 7 are expressed

Table 3. Linearity data obtained by least squares regression.

Analyte	Matrix	Equation of the line		R	R^2
		Angular coefficient	Linear coefficient		
Cu	H_2O	Y=1.0223x	$8x10^{-4}$	0.9983	0.9966
Fe	H_2O	Y=0.4405x	$3x10^{-4}$	0.9988	0.9980
Cu	Ethanol	Y=1.0420x	$3x10^{-6}$	0.9996	0.9992
Fe	Ethanol	Y=0.1290x	$1x10^{-4}$	0.9984	0.9969

Table 4. Coefficients of variation of the means of the SWASV peaks obtained and the coefficient of variation of Horwitz.

Matrix H_2O	Level of fortification ($mg.L^{-1}$)	CV Medium (%)	HCV (%)
BDD/Cu	0.001	0.2859	5.65
	0.004	0.3146	4.58
	0.007	0.4731	4.21
BDD/Fe	0.001	0.2516	5.65
	0.004	0.6293	4.58
	0.007	0.2744	4.21

Table 5. Coefficients of variation of the means of the SWASV peaks obtained and the coefficient of variation of Horwitz.

Matrix Ethanol	Level of fortification ($mg.L^{-1}$)	CV Medium (%)	HCV (%)
BDD/Cu	0.001	0.1424	5.65
	0.004	0.1116	4.58
	0.007	0.6388	4.21
BDD/Fe	0.001	0.4289	5.65
	0.004	0.6380	4.58
	0.007	0.2653	4.21

Table 6. Concentrations calculated from low, medium and high concentration control curves and recovery percentages of metals of interest in aqueous and ethanolic media.

Matrix H_2O	Point ($mg.L^{-1}$)	Conc. of the curve ($mg.L^{-1}$)	%R
BDD Cu	white	0.00179	-
	0.001	0.00268	89
	0.004	0.00593	103.5
	0.007	0.00896	102.4
BDD Fe	white	0.00113	-
	0.001	0.00206	93
	0.004	0.00499	96.5
	0.007	0.00855	106

the concentrations calculated from the analytical curves and the percentages of recovery calculated as described in the validation of the work methodology.

For the accuracy tests of this work the calculated recovery percentage is expected to be within the range of 70 to 110% stipulated by the AOAC (Association of Official Analytical Chemistry)[28]. The representations of recovery percentages calculated at low (0.001 $mg.L^{-1}$), mean (0.004 $mg.L^{-1}$) and high (0.007 $mg.L^{-1}$) concentration presented a satisfactory recovery percentage, once which fit within expected range (Table 6 and 7).

Considering that the CV results obtained during the precision test in terms of intraday repeatability were less than 10% and that the results obtained for the accuracy test in terms of percent recovery were within the predicted range, as recommended in literature[13], it is concluded that the method presents satisfactory precision and accuracy, thus guaranteeing reliability to the results obtained by the proposed method.

As described previously, the lowest concentration measured by the renucleated electrode was 0.0005 $mg.L^{-1}$ of Cu^{2+} and Fe^{3+}. To obtain the LD and LQ results a first study was carried out comparing these limits in aqueous and ethanolic media in distilled water and ethanol P.A., and then compared with the study carried out in the matrices. This study was necessary to know first the minimum amount detectable by the electrode and second to obtain the minimum detectable concentration in the matrix, since it has a significant amount of the analysed analytes, being necessary to perform dilutions in the matrices before doing the study of the LD and LQ[13]. Thus, the values of LD and LQ for metals Cu^{2+} and Fe^{3+} by the proposed voltammetric method can be observed in Table 8.

Table 7. Concentrations calculated from low, medium and high concentration control curves and recovery percentages of metals of interest in aqueous and ethanolic media.

Matrix Ethanol	Point ($mg.L^{-1}$)	Conc. of the curve ($mg.L^{-1}$)	%R
BDD Cu	white	0.00116	-
	0.001	0.00221	105
	0.004	0.00458	85.5
	0.007	0.00745	89.5
BDD Fe	white	0.00107	-
	0.001	0.00217	110
	0.004	0.00515	102
	0.007	0.00756	92.7

Table 8. LD and LQ obtained for the BDD micro/nano electrode in water and ethanol.

Electrode	Matrix	Metal	LD	LQ
BDD	H_2O	Cu	$2.69x10^{-4}$	$3.39x10^{-4}$
		Fe	$2.97x10^{-4}$	$3.26x10^{-4}$
	Ethanol	Cu	$4.92x10^{-4}$	$5.13x10^{-4}$
		Fe	$4.26x10^{-4}$	$4.87x10^{-4}$

The results showed lower values of LD and LQ for this electrode in aqueous medium, this is due to the fact that the matrix difference directly influences the data acquisition. However, considering the magnitude of the results obtained by this method, it was possible to confirm that it has satisfactory detection capacity and quantification efficiency.

4. Conclusions

The validation of the SWV technique using an electrode of mixed morphology provided positive values for the determination of metallic species on the surface of the BDD electrode. This proposed electroanalytical method, combined with the morphology of the BDD electrode, is an excellent candidate for use in the determination of metallic species in ethanol fuel and aqueous media, without the need for sample treatment. Standing out more strongly in the determination of metals in aqueous media, because of the matrix on the electrode surface. Studies on different film doping values, growth from the change in B/C ratio and physical modification of the BDD surface combined with detection in real samples need to be carried out to find even better results.

5. Acknowledgments

The authors gratefully acknowledge the CAPES, CNPq and FAPEAM (project FAPEAM N. 062.01142/2019), for financial assistance in performing the present research work.

6. References

1. Joshi P, Riley P, Goud KY, Mishra RK, Narayan R. Recent advances of boron-doped diamond electrochemical sensors toward environmental applications. Curr Opin Electrochem. 2021;32:100920. http://dx.doi.org/10.1016/j.coelec.2021.100920.
2. Li K, Yang H, Yuan X, Zhang M. Recent developments of heavy metals detection in traditional Chinese medicine by

atomic spectrometry. Microchem J. 2021;160:105726. http://dx.doi.org/10.1016/j.microc.2020.105726.
3. Nouari M, Frecha M, Bellil A. Study by absorption and emission spectrophotometry of the efficiency of the binary mixture (Ethanol-Water) on the extraction of betanin from red beetroot. Spectrochim Acta A Mol Biomol Spectrosc. 2021;260:119939. http://dx.doi.org/10.1016/j.saa.2021.119939.
4. Wang M, Yang T, Rao Y, Wang Z, Dong X, Zhang L, et al. A review on traditional uses, phytochemistry, pharmacology, toxicology and the analytical methods of the genus Nardostachys. J Ethnopharmacol. 2021;208:114446. http://dx.doi.org/10.1016/j.jep.2021.114446.
5. Shanmugam R, Alagumalai KP, Chen S, Ganesan T. Electrochemical evaluation of organic pollutant estradiol in industrial effluents. J Environ Chem Eng. 2021;9(4):105723. http://dx.doi.org/10.1016/j.jece.2021.105723.
6. Jiang X, Zhu Q, Zhu H, Zhu Z, Miao X. Antifouling lipid membrane coupled with silver nanoparticles for electrochemical detection of nucleic acids in biological fluids. Anal Chim Acta. 2021;1177:338751. http://dx.doi.org/10.1016/j.aca.2021.338751.
7. Baluchová S, Daňhel A, Dejmková H, Ostatná V, Fojta M, Schwarzová-Pecková K. Recent progress in the applications of boron doped diamond electrodes in electroanalysis of organic compounds and biomolecules – A review. Anal Chim Acta. 2019;1077:30-66. http://dx.doi.org/10.1016/j.aca.2019.05.041.
8. Wang Y, Wang W, Yang S, Shu G, Dai B, Zhu J. Two extreme crystal size scales of diamonds, large single crystal and nanocrystal diamonds: Synthesis, properties and their mutual transformation. N Carbon Mater. 2021;36(3):512-26. http://dx.doi.org/10.1016/S1872-5805(21)60030-6.
9. Sardinha A, Arantes T, Cristovan F, Ferreira N. From micro to nanocrystalline boron doped diamond applied to cadmium detection. Thin Solid Films. 2017;625:70-80. http://dx.doi.org/10.1016/j.tsf.2017.01.051.
10. Raposo F, Ibelli-Bianco C. Performance parameters for analytical method validation: controversies and discrepancies among numerous guidelines. Trends Analyt Chem. 2020;129:115913. http://dx.doi.org/10.1016/j.trac.2020.115913.
11. Bansod B, Kumar T, Thakur R, Rana S, Singh I. A review on various electrochemical techniques for heavy metal ions detection with different sensing platforms. Biosens Bioelectron. 2017;94:443-55. http://dx.doi.org/10.1016/j.bios.2017.03.031.
12. Kim S, Kim H, Kim S, Choi H, Pak S, Han S. Validation of analytical method for (E)-2-decenedioic acid quantification in honey samples. J Asia Pac Entomol. 2021;24(4):1153-7. http://dx.doi.org/10.1016/j.aspen.2021.10.013.
13. Konieczka P, Namiesnik J. Quality assurance and quality control in the analytical chemical laboratory. 2nd ed. Boca Raton: CRC Press; 2018.
14. International Organization for Standardization – ISO. ISO 12787:2011: cosmetics: analytical methods: validation criteria for analytical results using chromatographic techniques [Internet]. Geneva: ISO; 2011 [cited 2022 Sep 13]. Available from: https://www.iso.org/standard/51709.html
15. Shrivastava A, Saxena P. Validation of analytical methods: methodology and statistics. 1st ed. New Delhi: CBS Publishers and Distributors; 2017.
16. Rehacek V, Hotovy I, Marton M, Mikolasek M, Michniak P, Vincze A, et al. Voltammetric characterization of boron-doped diamond electrodes for electroanalytical applications. J Electroanal Chem. 2020;862:114020. http://dx.doi.org/10.1016/j.jelechem.2020.114020.
17. Deshmukh S, Sankaran K, Korneychuk S, Verbeeck J, McLaughlin J, Haenen K, et al. Nanostructured nitrogen doped diamond for the detection of toxic metal ions. Electrochim Acta. 2018;18:315688. http://dx.doi.org/10.1016/j.electacta.2018.07.067.
18. Volodin VA, Mortet V, Taylor A, Remes Z, Stuchliková TH, Stuchlik J. Raman scattering in boron doped nanocrystalline diamond films: manifestation of Fano interference and phonon confinement effect. Solid State Commun. 2018;276:33-6. http://dx.doi.org/10.1016/j.ssc.2018.04.004.
19. Pleskov YV, Evstefeeva YE, Krotova MD, Lim PY, Shih HC, Varnin VP, et al. Synthetic diamond electrodes: the effect of surface microroughnesson the electrochemical properties of CVD diamond thin films on titanium. J Appl Electrochem. 2005;35(9):857-64. http://dx.doi.org/10.1007/s10800-005-2572-0.
20. YYang W, Tan J, Chen Y, Li Z, Liu F, Long H, et al. Relationship between substrate type and BDD electrode structure, performance and antibiotic tetracycline mineralization. J Alloys Compd. 2022;890:161760. http://dx.doi.org/10.1016/j.jallcom.2021.161760.
21. Pei J, Yu X, Wei S, Boukherroub R, Zhang Y. Double-side effect of B/C ratio on BDD electrode detection for heavy metal ion in water. Sci Total Environ. 2021;771:145430. http://dx.doi.org/10.1016/j.scitotenv.2021.145430.
22. Shi C, Li C, Li M, Li H, Dai W, Wu Y, et al. Fabrication of porous boron-doped diamond electrodes by catalytic etching under hydrogen–argon plasma. Appl Surf Sci. 2016;360:315-22. http://dx.doi.org/10.1016/j.apsusc.2015.11.028.
23. Niu Y, Sun F, Xu Y, Cong Z, Wang E. Applications of electrochemical techniques in mineral analysis. Talanta. 2014;127:211-8. http://dx.doi.org/10.1016/j.talanta.2014.03.072.
24. Bansod B, Kumar T, Thakur R, Rana S, Singh I. A review on various electrochemical techniques for heavy metal ions detection with different sensing platforms. Biosens Bioelectron. 2017;94:443-55. http://dx.doi.org/10.1016/j.bios.2017.03.031.
25. Knight DS, White WB. Characterization of diamond films by Raman spectroscopy. J Mater Res. 2011;4(2):385-93. http://dx.doi.org/10.1557/JMR.1989.0385.
26. Volodin VA, Mortet V, Taylor A, Remes Z, Stuchliková TH, Stuchlik J. Raman scattering in boron doped nanocrystalline diamond films: manifestation of Fano interference and phonon confinement effect. Solid State Commun. 2018;276:33-6. http://dx.doi.org/10.1016/j.ssc.2018.04.004.
27. Xu K, Pérez-Ràfols C, Cuartero M, Crespo GA. Electrochemical detection of trace silver. Electrochim Acta. 2021;374:137929. http://dx.doi.org/10.1016/j.electacta.2021.137929.
28. Miranda L, Felsner ML, Torres YR, Hoss I, Galli A, Quináia SP. In-house validation of methyltestosterone determination in natural waters by voltammetry using hanging mercury drop electrode. Quim Nova. 2015;38:419-26. http://dx.doi.org/10.5935/0100-4042.20150014.